Transition State Structure and Rate Determination for the Acylation Stage of Acetylcholinesterase Catalyzed Hydrolysis of (Acetylthio)choline

ARTICLE *in* JOURNAL OF THE AMERICAN CHEMICAL SOCIETY · MARCH 2000

Impact Factor: 12.11 · DOI: 10.1021/ja9933590

Transition State Structure and Rate Determination for the Acylation Stage of Acetylcholinesterase Catalyzed Hydrolysis of (Acetylthio)choline

Siobhan Malany,[†,#] Monali Sawai,[†] R. Steven Sikorski,[†] Javier Seravalli,[†,⊥] Daniel M. Quinn,*[,†] Zoran Radić,[‡] Palmer Taylor,[‡] Chanoch Kronman,[§] Baruch Velan,[§] and Avigdor Shafferman[§]

Contribution from the Department of Chemistry, The University of Iowa, Iowa City, Iowa 52242, Department of Pharmacology, University of California-San Diego, La Jolla, California 92093, and Israel Institute for Biological Research, Ness-Ziona 70450, Israel

Received September 15, 1999

Abstract: Rate-limiting steps and transition state structure for the acylation stage of acetylcholinesterase-catalyzed hydrolysis of (acetylthio)choline have been characterized by measuring substrate and solvent isotope effects and viscosity effects on the bimolecular rate constant k_E ($=k_{cat}/K_m$). Substrate and solvent isotope effects have been measured for wild-type enzymes from *Torpedo californica*, human and mouse, and for various active site mutants of these enzymes. Sizable solvent isotope effects, $^{D_2O}k_E \sim 2$, are observed when substrate β-deuterium isotope effects are most inverse, $^{\beta D}k_E = 0.95$; conversely, reactions that have $^{D_2O}k_E \sim 1$ have substrate isotope effects of $^{\beta D}k_E = 1.00$. Proton inventories of k_E provide a quantitative measure of the contributions by the successive steps, diffusional encounter of substrate with the active site and consequent chemical catalysis, to rate limitation of the acylation stage of catalysis. For reactions that have the largest solvent isotope effects and most inverse substrate isotope effects, proton inventories are linear or nearly so, consistent with prominent rate limitation by a chemical step whose transition state is stabilized by a single proton bridge. Reactions that have smaller solvent isotope effects and less inverse substrate isotope effects have nonlinear and upward bulging proton inventories, consistent with partial rate limitations by both diffusional encounter and chemical catalysis. Curve fitting of such proton inventories provides a measure of the commitment to catalysis that is in agreement with the effect of solvent viscosity on k_E and with the results of a double isotope effect measurement, wherein $^{\beta D}k_E$ is measured in both H_2O and D_2O. The results of these various experiments not only provide a model for the structure of the acylation transition state but also establish the validity of solvent isotope effects as a tool for quantitative characterization of rate limitation for acetylcholinesterase catalysis.

Introduction

The physiological reaction catalyzed by acetylcholinesterase (AChE[1]) is the hydrolysis of the neurotransmitter acetylcholine (ACh). This reaction proceeds, after reversible substrate binding, by successive acylation and deacylation steps, as outlined in the following kinetic mechanism:

$$E + A \underset{k_2}{\overset{k_1}{\rightleftharpoons}} EA \xrightarrow{k_3} F + P \xrightarrow[H_2O]{k_5} E + Q$$

E, A, EA, and F are the free enzyme, free substrate, Michaelis complex, and the acylenzyme intermediate, respectively, and P and Q are the successive choline and acetate products. The bimolecular rate constant k_E ($\equiv k_{cat}/K_m$) for this mechanism is given by eq 1:

$$k_E = \frac{k_1 k_3}{k_2 + k_3} \quad (1)$$

The rate constant k_E is obtained by dividing the pseudo-first-order rate constant V_{max}/K_m by $[E]_T$, and therefore kinetic isotope and other effects on V_{max}/K_m are effects on k_E. As eq 1 shows, k_E is a function of microscopic rate constants that convert the free E + free A reactant state to the successive transition states of the substrate binding step (rate constant k_1) and the chemical step that produces the acylenzyme intermediate (rate constant k_3). As for many enzymes whose catalytic power is highly evolved, k_E for AChE approximates[2] the diffusion-controlled limit of Eigen and Hammes.[3] Because of this, k_E, which is frequently referred to as the observed acylation rate constant,

* To whom correspondence should be addressed: 319-335-1335 (phone); 319-335-1270 (fax); daniel-quinn@uiowa.edu.

† The University of Iowa.

Current address: Department of Pharmacology, University of California-San Diego, La Jolla, CA 92093.

⊥ Current address: Department of Biochemistry, University of Nebraska, The Beadle Center N113, Lincoln, NE 68588.

‡ University of California-San Diego.

§ Israel Institute for Biological Research.

(1) Abbreviations: ACh, acetylcholine; AChE, acetylcholinesterase; Ala, alanine; ATCh, (acetylthio)choline; DTNB, 5,5′-dithiobis(2-nitrobenzoic acid); Glu, glutamate; Gln, glutamine; His, histidine; HuAChE, human AChE.; MAChE, mouse AChE; Ser, serine; TcAChE, *Torpedo californica* AChE; TX100, Triton X-100.

(2) (a) Bazelyansky, M.; Robey, E.; Kirsch, J. F. *Biochemistry* **1986**, *25*, 125−130. (b) Hasinoff, B. B. *Biochim. Biophys. Acta* **1982**, *704*, 52−58. (c) Nolte, H.-J.; Rosenberry, T. L.; Neumann, E. *Biochemistry* **1980**, *19*, 3705−3711. (d) Quinn, D. M. *Chem. Rev.* **1987**, *87*, 955−979.

(3) Eigen, M.; Hammes, G. G. *Adv. Enzymol. Relat. Subj. Biochem.* **1963**, *25*, 1−38.

10.1021/ja9933590 CCC: $19.00
Published on Web 03/16/2000

Table 1. Isotope and Viscosity Effects for Wild-Type and Mutant AChEs

enzyme	relative k_e[a]	$^{D_2O}k_E$[b]	$^{\beta D}k_E$[b]	C[c]	$^{D_2O}k_3$[c]	$^{\beta D}k_{3E}$[d]
T. californica wild-type	1.0	1.47 ± 0.06	1.00 ± 0.01			
T. californica Glu199Gln	0.01	2.08 ± 0.07	0.98 ± 0.01			
human wild-type	0.07	1.62 ± 0.04	0.97 ± 0.01[e]	3 ± 1	3.0 ± 0.6	0.85 ± 0.06
			0.95 ± 0.01[e]	1.2 ± 0.2[f]		0.88 ± 0.04
human Glu202Gln	0.009	1.84 ± 0.08	0.96 ± 0.02	1.8 ± 0.3	3.1 ± 0.5	0.87 ± 0.06
human Glu202Ala	0.0004	2.1 ± 0.1	0.95 ± 0.02	0.4 ± 0.2	2.4 ± 0.4	0.93 ± 0.03
mouse wild-type	0.05	1.26 ± 0.04	1.000 ± 0.005	∞[g]		
mouse Glu202Gln	0.001	1.5 ± 0.1	0.97 ± 0.01			

[a] Relative k_E values were obtained by dividing measured k_E values by the $k_E = 1.0 \times 10^9\ M^{-1}\ s^{-1}$ for *T. californica* AChE. All k_E values for these comparisons were extrapolated to zero ionic strength, as described by Quinn et al.[34] [b] Parameters were measured at 25.0 ± 0.2 °C in the following buffers: TcAChE, 0.1 M sodium phosphate buffer, pH 7.16 and pD 7.78, $\mu = 0.22$; HuAChE, 0.1 M sodium phosphate buffer, pH 7.30 and pD 7.80, $\mu = 0.35$; MAChE, 0.04 M sodium phosphate buffer, pH 7.50 and pD 8.10, $\mu = 0.10$. [c] Except where indicated (see footnote f), commitment values and intrinsic solvent isotope effects were calculated by fitting proton inventories to eq 4 of the text, as demonstrated in Figure 1. For the wild-type human AChE reaction, the commitment in D_2O was estimated in the text as $C^{D_2O} = 1.2 \pm 0.5$. [d] Calculated according to eq 7, as explained in the text. [e] The respective isotope effects were measured in buffered H_2O and D_2O. The Student t-test indicates that the isotope effects are different at the 99.5% confidence level. [f] Determined from dependence of k_E on solvent viscosity; see Figure 2. [g] Curve-fitting of viscosity dependencies as in Figure 2 gave very large values of C ($>10^5$), consistent with sole rate limitation by substrate binding, i.e. k_1.

is not likely to be rate limited by just one of the successive transition states.

The surrogate substrate (acetylthio)choline (ATCh) provides a convenient alternative to the physiological substrate ACh, since hydrolysis of ATCh can be monitored by the sensitive and continuous spectrophotometric Ellman assay.[4] The values of k_{cat} and k_{cat}/K_m for *Electrophorus electricus* AChE-catalyzed hydrolyses of the two substrates are nearly identical,[2d] and k_{cat} values for the two substrates are rate-limited by acylation and deacylation to comparable extents.[5] Consequently, AChE catalysis is impervious to the O→S elemental substitution in the etherial position of the ester function of the substrate.

A reasonable strategy for increasing the rate limitation of k_E by the k_3 step is to utilize mutant AChEs in which the effect of mutation is to selectively destabilize the transition state of the chemical step. Shafferman et al.[6] suggest that reductions in k_E that accompany replacement of Glu202 of the active site of human AChE with Gln, Ala, or Asp arise from slowing of the acylation step k_3, and ascribe this effect to disruption in the mutant enzymes of an H-bond network that positions catalytic and ligand binding residues. For the corresponding Glu199 to Gln mutant of *Torpedo californica* AChE, Radić et al.[7] also suggests that the catalytic efficiency is affected. Consequently, Glu202(*199*)[8] mutants are utilized herein to increase rate limitation by the chemical step in the acylation stage of AChE catalysis.

In this article, we describe the results of solvent and substrate isotope effects and viscosity effects on k_E for hydrolysis of ATCh catalyzed by wild-type and mutant AChEs from *Torpedo californica* (TcAChE), human (HuAChE), and mouse (MAChE). These distinct experimental approaches provide complementary information that allows postulation of a model for the geometry of the acylation transition state. Implicit in the analyses described herein is that mammalian and marine AChEs have transition states that are structurally similar. This assumption is supported by the observations that the active sites of *T. californica* and mouse AChEs are similarly situated in the enzyme interiors at the bottom of 20 Å deep active site gorges, and that the amino acids that line the gorges are highly conserved.[9] Solvent isotope effect measurements in mixed H_2O-D_2O buffers (called proton inventories[10]) provide a quantitative accounting of rate limitation in the acylation stage of catalysis. The results of proton inventory experiments are corroborated by substrate isotope and viscosity effects. Correlations between these different experimental approaches establish the validity of solvent isotope effects as a tool for characterizing the dynamics of AChE catalysis.

Results and Discussion

Isotope Effect Comparisons for Wild-Type and Mutant Enzymes. Table 1 lists the results of isotope effect and viscosity experiments on various AChEs. Solvent isotope effects are expressed as the ratio of k_E values measured in equivalently buffered solutions of H_2O and D_2O,[11] *i.e.* $^{D_2O}k_E = k_E^{H_2O}/k_E^{D_2O}$; β-deuterium isotope effects are ratios of k_E values for hydrolyses of (acetyl-$^1H_3$-thio)choline and (acetyl-$^2H_3$-thio)choline; i.e. $^{\beta D}k_E = k_E^{H3}/k_E^{D3}$. For AChEs from each of the species in Table 1, there is a striking correlation between solvent and substrate isotope effects. The larger the solvent isotope effect, the more inverse (i.e. less than unity) is the β-deuterium isotope effect.

(4) Ellman, G. L.; Courtney, K. D.; Andres, J. V.; Featherstone, R. M. *Biochem. Pharmacol.* **1961**, *7*, 88−95.

(5) Froede, H. C.; Wilson, I. B. *J. Biol. Chem.* **1984**, *259*, 11010−11013.

(6) (a) Shafferman, A.; Ordentlich, A.; Barak, D.; Kronman, C.; Ariel, N.; Velan, B. In *Structure and Function of Cholinesterases and Related Proteins*; Doctor, B. P., Taylor, P., Quinn, D. M., Rotundo, R. L., Gentry, M. K., Eds.; Plenum Press: New York and London, 1999; pp 203−209. (b) Shafferman, A.; Ordentlich, A.; Barak, D.; Stein, D.; Ariel, N.; Velan, B. *Biochem. J.* **1996**, *318*, 833−840.

(7) Radić, Z.; Gibney, G.; Kawamoto, S.; MacPhee-Quigley, K.; Bongiorno, C.; Taylor, P. *Biochemistry* **1992**, *31*, 9760−9767.

(8) The sequence positions of amino acid residues are denoted by two numbers. The first number in normal type is the sequence position in mammalian AChE, and the number in italics and parentheses is the sequence position in *Torpedo californica* AChE. This dual numbering scheme follows the convention proposed in the following reference: Massoulié, J.; Sussman, J. L.; Doctor, B. P.; Soreq, H.; Velan, B.; Cygler, M.; Rotundo, R.; Shafferman, A.; Silman, I.; Taylor, P. In *Multidiscliplinary Approaches to Cholinesterase Functions*; Shafferman, A., Velan, B., Eds.; Plenum Press: New York and London, 1992; pp 285−288.

(9) (a) The crystal structure of *Torpedo californica* AChE was first described by Sussman and colleagues: Sussman, J. L.; Harel, M.; Frolow, F.; Oefner, C.; Goldman, A.; Toker, L.; Silman, I. *Science* **1991**, *253*, 872−879. (b) The crystal structure of the complex of mouse AChE and the snake venom toxin fasciculin is found in the following: Bourne, Y.; Taylor, P.; Marchot, P. *Cell* **1995**, *83*, 503−512. (c) Gentry and Doctor have compared the primary sequences of various esterases of the α/β hydrolase fold supergene family, which includes AChE: Gentry, M. K.; Doctor, B. P. In *Enzymes of the Cholinesterase Family*; Quinn, D. M., Balasubramanian, A. S., Doctor, B. P., Taylor, P., Eds.; Plenum Press: New York and London, 1995; pp 493−505.

(10) (a) Quinn, D. M.; Sutton, L. D. In *Enzyme Mechanism from Isotope Effects*; Cook, P. F., Ed.; CRC Press: Boca Raton, 1991; pp 73−126. Additional references to solvent isotope effect reviews can be found in this article. (b) Kiick has discussed the relationship between the curvature of proton inventories and commitment factors that are in turn estimated from substrate isotope effects: Kiick, D. M. *J. Am. Chem. Soc.* **1991**, *113*, 8499−8504.

(11) Equivalent H_2O and D_2O buffers are those that contain the same concentrations of all solutes.

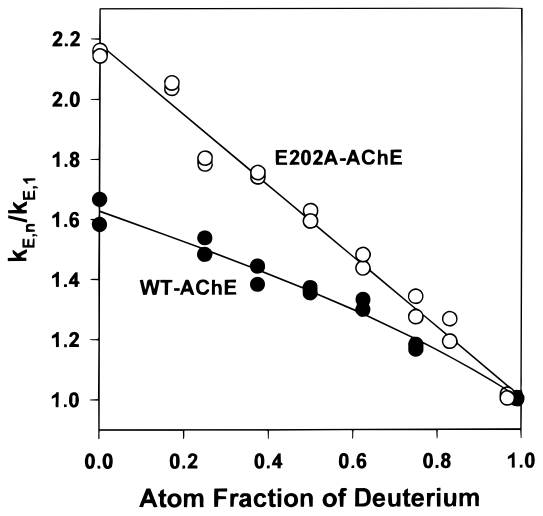

Figure 1. Proton inventories for k_E of human AChE-catalyzed hydrolysis of ATCh. Reactions were monitored as described in the Enzyme Kinetics and Data Analysis subsection in the Experimental Section. Filled-circles are for wild-type AChE and arise from following first-order time courses in 0.1 M sodium phosphate buffer, pH 7.34 in H_2O and pD 7.86 in D_2O, that contained sufficient NaCl so that $\mu = 0.35$; reactions also contained 190 pM AChE, 2 mM TX100, 0.5 mM DTNB, and $[ATCh]_0 = 25$ μM ($=K_m/12$). Open circles are for the Glu202(*199*)Ala mutant and arise from initial rate measurements in 0.01 M sodium phosphate buffer, pH 7.26 in H_2O and pD 7.86 in D_2O, that contained sufficient NaCl so that $\mu = 0.1$; reactions also contained 2.0 nM AChE, 2 mM TX100, 0.5 mM DTNB, and 31 μM ATCh ($=K_m/50$). The solid lines are least-squares fits to eq 4; the corresponding parameters for wild-type AChE are $\phi_3^T = 0.33 \pm 0.06$ and $C = 3 \pm 1$, and for Glu202(*199*)Ala AChE the parameters are $\phi_3^T = 0.39 \pm 0.06$ and $C = 0.4 \pm 0.3$.

For ester hydrolysis inverse β-deuterium effects arise from partial sp^2 to sp^3 rehybridization of the carbonyl carbon as the reactant state is converted into the transition state.[12] Consequently, the correlation of increasingly inverse β-deuterium effects with increasingly normal (i.e. greater than unity) solvent isotope effects suggests that mutant AChEs that react more slowly, as manifested by relative k_E values, do so with greater rate limitation by the chemical step k_3.

Solvent Isotope Effects and Acylation Reaction Dynamics. A quantitative accounting of acylation reaction dynamics can be had by conducting proton inventories of k_E, as shown in Figure 1. In these experiments k_E is measured as a function of the atom fraction of deuterium in mixed isotopic buffers. The respective substrate binding and release rate constants k_1 and k_2 are diffusion controlled, and therefore should be slower in D_2O than in H_2O by a factor of 1.2, the relative viscosities of the two solvents.[10a] The following pair of equations suggests that the dependence of these rate constants on the atom fraction of deuterium n in mixed isotopic solvents arises from a medium effect:[10a,13]

$$k_{1n} = 1.2^{-n} k_1^{H_2O} \qquad k_{2n} = 1.2^{-n} k_2^{H_2O} \tag{2}$$

The k_3 step is that for nucleophilic attack of Ser203(*200*)[8] on the carbonyl carbon of the substrate, with concomitant proton transfer from Ser203(*200*)[8] to His447(*440*)[8] in the active site triad.[14] This single proton bridge gives rise to a linear dependence of k_3 on n:[15]

$$k_{3,n} = k_3^{H_2O}(1 - n + n\phi_3^T) \tag{3}$$

Substitution of eqs 2 and 3 into eq 1 gives the following equation for proton inventories of k_E:

$$k_{E,n} = k_E^{H_2O} \frac{(1 + C)(1 - n + n\phi_3^T)}{1 + 1.2^n C(1 - n + n\phi_3^T)} \tag{4}$$

In this equation $k_{E,n}$ and $k_E^{H_2O}$ are the values of k_E in H_2O-D_2O mixtures of atom fraction of deuterium n and 0, respectively; ϕ_3^T is the fractionation factor of the bridging proton that stabilizes the transition state of the k_3 step, and C ($=k_3/k_2$) is the commitment to catalysis.[16] The intrinsic isotope effect on the k_3 step is $^{D_2O}k_3 = 1/\phi_3^T$. Figure 1 shows that the Glu202Ala mutant of HuAChE, which according to Table 1 gives the most inverse β-deuterium and the largest solvent isotope effects, yields a nearly linear proton inventory. Equation 4 predicts a linear dependence when $C = 0$, i.e. when the k_3 step is solely rate limiting.[17] The average parameters of three such proton inventories are $C = 0.4 \pm 0.2$ and $^{D_2O}k_3 = 2.4 \pm 0.4$. The average commitment is consistent with $70 \pm 10\%$ rate limitation by the k_3 step,[17] and the magnitude of the intrinsic solvent isotope effect is reasonable for a step whose transition state is stabilized by O to N proton transfer from Ser203(*200*) to His447(*440*).[10a] On the other hand, wild-type HuAChE gives a proton inventory that is nonlinear and upward bulging, as also shown in Figure 1. Least-squares analysis of this proton inventory gives $^{D_2O}k_3 = 3.0 \pm 0.6$ and $C = 3 \pm 1$, and therefore the k_3 step is now only $25 \pm 8\%$ rate limiting. These results are consistent with the less inverse β-deuterium isotope effect and smaller solvent isotope effect for the wild-type enzyme than for the Glu202Ala mutant. Moreover, the intrinisic solvent isotope effect $^{D_2O}k_3$ for the wild-type enzyme is similar to that for the Glu202Ala mutant, which supports the internal consistency of the model described herein for AChE acylation reaction dynamics.

Viscosity Effects and Acylation Reaction Dynamics. The effect of viscosity of the reaction medium on k_E, plotted in Figure 2, supports the quantitative model for acylation reaction dynamics presented above. As the viscosity η_{rel} increases, the respective rate constants k_1 and k_2 for substrate binding and release decrease:[18] $k_{1\eta} = k_1/\eta_{rel}$ and $k_{2\eta} = k_2/\eta_{rel}$. Incorporation

(12) (a) Hogg, J. L. In *Transition States of Biochemical Processes*; Gandour, R. D., Schowen, R. L., Eds.; Plenum Press: New York, 1978; pp 201−224. (b) Kovach, I. M.; Belz, M.; Larson, M.; Rousy, S.; Schowen, R. L. *J. Am. Chem. Soc.* **1985**, *107*, 7360−7365.

(13) Mata-Segreda has reported that the viscosity of mixed isotopic waters is a quadratic function of n: Mata-Segreda, J. F. *Rev. Latinoam. Quim.* **1979**, 151−153. Use of a quadratic dependence for k_1 and k_2 in eq 4 instead of a medium effect has no significant effect on the least-squares estimates of C and ϕ_3^T.

(14) Quinn, D. M.; Feaster, S. R. In *Comprehensive Biological Catalysis*; Sinnott, M., Ed.; Academic Press: London, 1998; Vol. 1, pp 455−482.

(15) The following references provide precedents for linear proton inventories for the chemical steps of AChE catalysis: (a) Pryor, A. N.; Selwood, T.; Leu, L.-S.; Andracki, M. A.; Lee, B. H.; Rao, M.; Rosenberry, T.; Doctor, B. P.; Silman, I.; Quinn, D. M. *J. Am. Chem. Soc.* **1992**, *114*, 3896−3900. (b) Kovach, I. M.; Larson, M.; Schowen, R. L. *J. Am. Chem. Soc.* **1986**, *108*, 3054−3056. (c) Acheson, S. A.; Dedopoulou, D.; Quinn, D. M. *J. Am. Chem. Soc.* **1987**, *109*, 239−245.

(16) (a) Northrop, D. B. *Biochemistry* **1975**, *14*, 2644−2651. (b) Northrop, D. B. In *Isotope Effects on Enzyme-Catalyzed Reactions*; Cleland, W. W., O'Leary, M. H., Northrop, D. B., Eds.; University Park: Baltimore, 1977; pp 122−152.

(17) The fraction of rate limitation by the k_3 step is $f_3 = 1/(1 + C)$; cf. refs 2d and 10a.

(18) For a discussion of viscosity effects on enzyme reactions, including the effect of the greater viscosity of D_2O than of H_2O, see: Karsten, W. E.; Lai, C.-H.; Cook, P. F. *J. Am. Chem. Soc.* **1995**, *117*, 5914−5918.

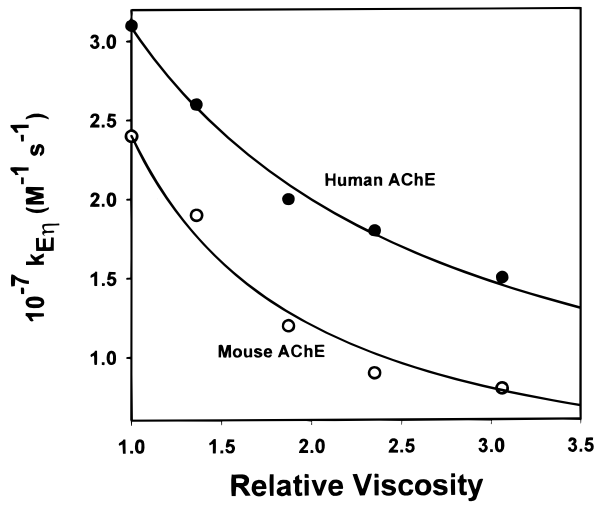

Figure 2. Viscosity effects on wild-type mouse and human AChE-catalyzed hydrolyses of ATCh. Values of k_E were measured by first-order kinetics in 0.05 M sodium phosphate buffer, pH 7.44, that contained various concentrations of glycerol, 0.3 mM DTNB, and 2 mM TX100. Solid circles are for reactions that contained 37 pM human AChE; k_E values were calculated by dividing V_{max}/K_m values, determined by fitting initial velocities to eq 11, by the enzyme concentration. Open circles are for reactions that contained 100 pM mouse AChE and $[ATCh]_0 = 10$ μM ($<K_m/10$); k_E values were determined by fitting first-order time courses to eq 12. The solid lines are fits to eq 5. For human AChE the corresponding least-squares parameters are $C = 1.2 \pm 0.2$ and $k_1 = 5.7 \pm 0.3 \times 10^7$ M^{-1} s^{-1}. For mouse AChE relative viscosity increases are matched by relative decreases in k_E, and therefore eq 5 reduces to $k_{E\eta} = k_1/\eta_{rel}$; from the least-squares fit $k_1 = (2.40 \pm 0.07) \times 10^7$ M^{-1} s^{-1}.

of these dependences into eq 1 gives:

$$k_{E\eta} = \frac{k_1 C}{1 + \eta_{rel} C} \tag{5}$$

Analysis of the viscosity dependence of Figure 2 according to eq 5 gives $C = 1.2 \pm 0.2$, which is consistent with $45 \pm 8\%$ rate limitation by the k_3 step. This result is in reasonable quantitative agreement with that derived from the proton inventory of Figure 1. Similar experiments for wild-type MAChE indicate that k_E is solely rate limited by the k_1 step, which is consistent with the diminutive solvent and β-deuterium isotope effects in Table 1. In fact, the solvent isotope effect on k_E for wild-type MAChE is just that expected to arise from the relative viscosities of H_2O and D_2O,[10a] as expected for a diffusion-controlled reaction.

Acylation Transition State Structure from β-Deuterium Isotope Effects. The effect of solvent isotope on the β-deuterium effect also supports the quantitative assessment of acylation reaction dynamics that derives from proton inventory experiments. Consider the $^{\beta D}k_E$ values of 0.97 ± 0.01 and 0.95 ± 0.01 for wild-type HuAChE reactions in H_2O and D_2O, respectively (cf. Table 1). The solvent isotope effect on the β-deuterium substrate isotope effect is consistent with the idea that the chemical k_3 step is subject to more sizable isotope effects than is the k_1 step, and that the k_3 step is more rate-limiting in D_2O than in H_2O. The analysis that follows shows how this information can be used to determine the intrinsic β-deuterium isotope effect, from which a model of the transition state of the k_3 step can be constructed.

The relationship between the observed β-D effect on k_E and the intrinsic β-D effect on the k_3 step is derived by writing versions of eq 1 for each of the isotopic substrates:

$$k_E^{H3} = \frac{k_1^{H3} k_3^{H3}}{k_2^{H3} + k_3^{H3}} \qquad k_E^{D3} = \frac{k_1^{D3} k_3^{D3}}{k_2^{D3} + k_3^{D3}} \tag{6}$$

Taking the ratio of these equations provides the following:

$$^{\beta D}k_E = \frac{^{\beta D}k_{3E} + {}^{\beta D}k_1 C}{1 + C} \tag{7}$$

In this equation $^{\beta D}k_{3E} = {}^{\beta D}k_1 {}^{\beta D}k_3/{}^{\beta D}k_2$, wherein $^{\beta D}k_1 = k_1^{H3}/k_1^{D3}$, for example. Therefore, $^{\beta D}k_{3E}$ is the intrinsic β-deuterium substrate isotope effect for conversion of the E + A reactant state to the transition state of the k_3 step. Similarly, $^{\beta D}k_1$ is the intrinsic isotope effect for diffusional encounter of AChE and ATCh. A reliable estimate of $^{\beta D}k_1$ is the following:[19]

$$^{\beta D}k_1 = \sqrt{\frac{\text{mass of (acetyl-}^2H_3\text{-thio)choline}}{\text{mass of (acetyl-}^1H_3\text{-thio)choline}}} = 1.009 \tag{8}$$

By using this value for $^{\beta D}k_1$ and values of the commitment to catalysis, C, that were determined in proton inventories, one can solve eq 7 for $^{\beta D}k_{3E}$. This procedure gives $^{\beta D}k_{3E} = 0.85 \pm 0.06$ for the wild-type human AChE-catalyzed hydrolysis of ATCh, as tabulated in Table 1. One can also calculate the intrinsic β-deuterium substrate isotope effect from the corresponding isotope effect that was measured in D_2O, i.e. $^{\beta D}k_E = 0.95 \pm 0.01$. The commitment in D_2O is calculated from the commitment in H_2O and the intrinsic solvent isotope effects on the k_2 and k_3 steps: $C^{D_2O} = {}^{D_2O}k_2 C^{H_2O}/{}^{D_2O}k_3 = 1.2(3 \pm 1)/(3.0 \pm 0.6) = 1.2 \pm 0.5$. Calculation according to eq 7 gives $^{\beta D}k_{3E} = 0.88 \pm 0.04$, in agreement with the value calculated for the reaction in H_2O. Therefore, the smaller observed β-D effect in H_2O than in D_2O arises from more prominent rate limitation by the k_3 step in the latter than in the former solvent, and indicates that the k_3 step is more sensitive to solvent and substrate isotopic substitution than the k_1 and k_2 steps.

Intrinsic β-deuterium substrate isotope effects were also calculated for reactions of the Glu202Gln and Glu202Ala mutants of human AChE. The weighted average of the four intrinsic substrate isotope effects in Table 1 is $^{\beta D}k_{3E} = 0.90 \pm 0.03$. This average effect can be used to estimate the fractional change (f) in hybridization ($sp^2 \rightarrow sp^3$) of ATCh and the bond order between the γO of Ser203(*200*) and the carbonyl carbon of ATCh in the transition state:[12b]

$$^{\beta D}k_{3E} = (^{\beta D}K_{eq})^f \tag{9}$$

The isotope effect $^{\beta D}K_{eq}$ is that for equilibrium addition to the carbonyl carbon, has a value of 0.87 for three deuteriums,[12b] and provides a measure of the effect expected for full $sp^2 \rightarrow sp^3$ rehybridization. The value calculated from this equation for the fractional change in hybridization is $f = 0.7_6 \pm 0.2_2$. The salient feature of this estimate is that the chemical transition state for the acylation stage of AChE-catalyzed hydrolysis of ATCh bears considerable structural resemblance to the putative tetrahedral intermediate. To provide a more quantitative view of the transition state, a gas-phase model of the tetrahedral intermediate for methoxide addition to carbonyl-protonated (acetylthio)choline was generated by ab initio quantum me-

(19) The modest normal β-deuterium isotope effect calculated according to eq 8 arises from the mass dependence of the frequency of collisions of the respective isotopic (acetylthio)cholines with the enzyme: Leffler, J. E.; Grunwald, E. *Rates and Equilibria in Organic Reactions*; John Wiley: New York and London, 1963; pp 57−59.

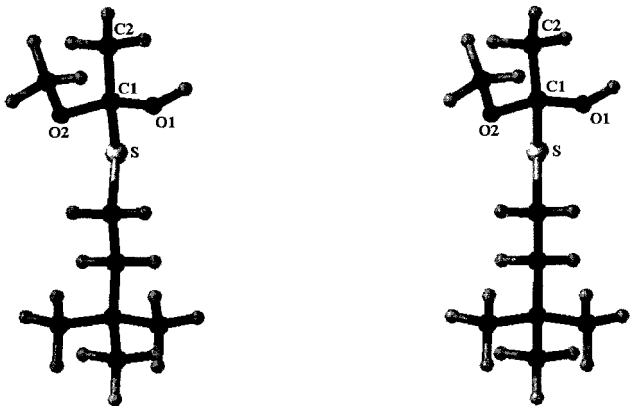

Figure 3. Crossed stereoview of a model for the transition state for methoxide addition to carbonyl-protonated (acetylthio)choline.

Table 2. Selected Structural Features of Protonated Ester, Tetrahedral Intermediate, and Transition State Models

parameter[a]	protonated ester	tetrahedral intermediate	transition state
C_1-O_1	1.261	1.386	1.379
C_1-O_2, Å		1.371	1.45[b]
C_1-C_2, Å	1.491	1.524	1.519
C_1-S, Å	1.707	1.851	1.839
C_2-C_1-S, deg	117.55	106.94	107.94
$C_2-C_1-O_2$, deg		114.17	112.96
$C_2-C_1-O_1$, deg	116.30	112.04	112.94
$O_1-C_1-O_2$, deg		107.42	106.63
O_1-C_1-S, deg	126.15	110.17	111.10
O_2-C_1-S, deg		105.91	105.03

[a] Parameters with two-atom designations (e.g. C_1-O_1) are bond distances, and those with three-atom designations (e.g. C_2-C_1-S) are bond angles. See Figure 3 for specification of atom labels. [b] Distance constrained as calculated according to eq 10 from the corresponding distance in the tetrahedral intermediate. Dihedral angle constraints are outlined in the Computational Modeling of the Transition State subsection in the Experimental Section.

chanical calculations.[20] This model possesses a nucleophilic oxygen to carbonyl carbon bond distance of 1.373 Å. Using this value as an estimate of the single bond distance, one can calculate the corresponding distance in the transition state from the following Pauling bond-order/bond-distance relationship:[21]

$$D(f) = D(1) - 0.6 \log(f) \qquad (10)$$

This calculation gives $D(f) = 1.45 \pm 0.05$ Å. The transition state model that is displayed in Figure 3 was then generated by constraining the nucleophilic methoxy oxygen−carbonyl carbon distance at 1.45 Å. Table 2 compares various bond lengths and angles for the tetrahedral intermediate and transition state models, as well as for the starting carbonyl-protonated ester. These data confirm the general impression that the transition state bears appreciable structural similarity to the tetrahedral intermediate, particularly with respect to bond angles in which the carbonyl carbon is the central atom.

Comparison with Other Theoretical Models. The experimental transition state structure described herein is in good agreement with theoretical models in the literature for the acylation transition state in AChE catalysis. Fuxreiter and Warshel[22] used the effective valence bond/free energy perturbation method to simulate the free energetics of formation of the tetrahedral intermediate in the acylation stage of AChE-catalyzed hydrolysis of acetylcholine and in the corresponding reaction in water. Their calculations suggest that on the enzyme the transition state lies 16 and 3.6 kcal mol^{-1} above the ester reactant and the tetrahedral intermediate, respectively. From these energetics one can estimate the fractional progress in the transition state as $f = 0.68$ by utilizing intersecting parabolas.[23] The agreement with our experimentally determined value, $f = 0.7_6 \pm 0.2_2$, is gratifying, in that both measures indicate that the transition state more closely resembles the tetrahedral intermediate than the reactant ester.

The quantum mechanical calculations of Wlodek et al.[24] for the formation of the tetrahedral intermediate in the acylation stage of AChE catalysis suggest a smaller fractional progress in the transition state than supported by the experiments described herein. However, their gas-phase model for acylation energetics understandably predicts that the tetrahedral intermediate is more stable than the reactant state. The efficacy of their calculations resides in the quantitative accounting they provide for the effect of the Glu202(*199*) to Gln mutation on the activity of AChE.[24]

Conclusion. Much has been made in recent years of the fact that amino acid side chains and peptide NH functions of enzymes have a wide range, $\phi = 0.3$ to 1.8, of proton fractionation factors.[25] This observation has been taken as impugning the ability of solvent isotope effects to produce useful information on transition state structure and reaction dynamics in enzyme-catalyzed reactions. The work detailed herein largely allays this concern for AChE catalysis. Three independent measures, viz. solvent and substrate isotope effects and viscosity effects, give reasonably the same picture of fractional rate limitation in the acylation stage of catalysis. The agreement of these three methods inspires confidence not only in the model for acylation reaction dynamics described herein but also in the integrity of solvent isotope effect measurements to provide quantitative information thereon.

Experimental Section

Materials. Reagents for the synthesis of isotopic (acetylthio)cholines were purchased from the following sources: 2-aminoethanethiol hydrochloride, $Na_2S\cdot 9H_2O$, $(^2H_3CCO)_2O$, dimethyl sulfate, and iodomethane, Aldrich Chemical Co.; $(^1H_3CCO)_2O$, EM Science. (Acetylthio)choline chloride, DTNB, $NaH_2PO_4\cdot H_2O$, $Na_2HPO_4\cdot 7H_2O$, and

(20) Frisch, M. J.; Trucks, G. W.; Schlegel, H. B.; Gill, P. M. W.; Johnson, B. G.; Robb, M. A.; Cheeseman, J. R.; Kieth, T. A.; Petersson, G. A.; Montgomery, J. A.; Raghavachari, K.; Al-Laham, M. A.; Zarkrzewski, V. G.; Ortiz, J. V.; Foresman, J. B.; Cioslowski, J.; Stefanov, B. B.; Nanayakkara, A.; Challocombe, M.; Peng, C. Y.; Ayala, P. Y.; Chen, W.; Wong, M. W.; Andres, J. L.; Replogle, E. S.; Gomperts, R.; Martin, R. L.; Fox, D. J.; Binkley, J. S.; Defrees, D. J.; Baker, J.; Stewart, J. P.; Head-Gordon, M.; Gonzalez C.; Pople, J. A. 1995**,** GAUSSIAN 94 (Revision D.4); Gaussian, Inc.: Pittsburgh, PA.

(21) Pauling, L. *The Nature of the Chemical Bond*, 3rd ed.; Cornel University Press: Ithaca, NY, 1960; pp 255−256.

(22) Fuxreiter, M.; Warshel, A. *J. Am. Chem. Soc.* **1998**, *120*, 183−194.

(23) Estimation of the fractional progress in the transition state from the reaction energetics is achieved by calculating the intersection point of two parabolas, each that have positive curvature. The minimum of one parabola is set at $f = 0$, where f is the fractional reaction progress, and $y = 0$, where y is the free energy in kcal mol^{-1}, i.e. $y = af^2$. The minimum of the second parabola is set at $f = 1$ and $y = 12.4$, which corresponds to the structure and energetics of the tetrahedral intermediate; this gives $y = a(f - 1)^2 + 12.4$. Since the free energy of the transition state is 16 kcal mol^{-1} above that of the reactant ester, y is set at 16 and the simultaneous equations are solved for $a = 34.8$ kcal mol^{-1} and $f = 0.68$.

(24) Wlodek, S. T.; Antosiewicz, J.; Briggs, J. M. *J. Am. Chem. Soc.* **1997**, *119*, 8159−8165.

(25) Loh, S. N.; Markley, J. L. *Biochemistry* **1994**, *33*, 1029−1036. A notable feature of the fractionation factors reported by Loh and Markley is that their average value is ∼0.8, which will generate a diminutive solvent isotope effect of ∼1.2. Moreover, unless there is a palpable shift from this value in the transition state of an enzymic reaction (a supposition for which there is no evidence), the wide variation of fractionation factors reported by Loh and Markley is of no relevance to the interpretation of solvent deuterium kinetic isotope effects.

Triton X-100 were purchased from Sigma Chemical Co. H_2O used in buffer preparation was distilled and subsequently deionized by passage through a Barnstead D8922 mixed-bed ion-exchange column (Sybron Corp). D_2O was used as purchased from Isotec Inc. Buffer salts were commercially available reagent grade materials. A Corning model 125 pH meter, equipped with a glass combination electrode, was used to measure buffer pH values. For D_2O buffers, pD values were determined by adding 0.4 to the pH meter reading.[10a]

Wild-type and mutant recombinant AChEs from *Torpedo californica*,[7] mouse,[26] and *homo sapiens*[27] were produced and characterized as described previously. Stock enzyme solutions were diluted in reaction buffers prior to use.

Synthesis of Isotopic (Acetylthio)cholines. Acetyl-$^2H_3$-thiocholine was synthesized as follows. 2-(*N*,*N*-Dimethylamino)ethanethiol was produced by successive additions of 1 equiv of dimethyl sulfate to 2-aminoethanethiol hydrochloride, as described by Nair et al. for the dimethylation of 3-bromoaniline.[28] 2-(*N*,*N*-Dimethylamino)ethanethiol hydrochloride (7.03 g, 50 mmol) was dissolved in aqueous sodium sulfide (40 mL, 0.6 M) and extracted with 3 × 25 mL of $CHCl_3$. $^2H_3$-acetic anhydride (2.69 g, 24.9 mmol) was added to the combined $CHCl_3$ extracts in a round-bottom flask, and the reaction mixture was stirred at room temperature for 4 h. The reaction mixture was washed with 3 × 10 mL of Na_2CO_3 (1.0 M); the aqueous extracts were combined, extracted with 10 mL of $CHCl_3$, dried over $MgSO_4$, filtered, and concentrated by rotary evaporation. Acetyl-$^2H_3$-thio-2-(*N*,*N*-dimethylamino)ethane was purified by fractional distillation (90−95 °C, ∼20 mmHg) in a short-path distillation apparatus. The final methylation was effected by slow addition with stirring of iodomethane (10.8 g, 70 mmol) to 1.97 g (13 mmol) of acetyl-$^2H_3$-thio-2-(*N*,*N*-dimethylamino)-ethane in dry acetone in a round-bottom flask. The highly exothermic reaction formed a precipitate almost immediately. The precipitate was collected by filtration, washed with dry Et_2O (40 mL), and dried in vacuo at room temperature to give acetyl-$^2H_3$-thiocholine as a white powder. High-resolution mass spectra, acquired on an AutoSpec spectrometer operated in the electron spray ionization mode, gave a molecular mass for $^2H_3CCOSCH_2CH_2N^+(CH_3)_3$ of 165.21 u (calculated 165.29 u), and indicated that the percent deuteration of the acetyl group was >97%. Proton NMR spectra, acquired at 300 MHz on an MSL-300 spectrometer, were consistent with the expected structure of the compound.

Enzyme Kinetics and Data Analysis. Reaction time courses for AChE-catalyzed hydrolysis of ATCh were monitored at 25.0 ± 0.2 °C by the Ellman assay,[4] which utilizes coupling of the thiocholine product with DTNB to generate a product that absorbs at $\lambda = 412$ nm ($\epsilon = 13600\ M^{-1}\ cm^{-1}$). Initial velocities were calculated by linear least-squares analysis of time courses for <10% turnover of the initial substrate concentration. The kinetic parameters K_m and V_{max} were determined by fitting initial velocities to the Michaelis−Menten equation:

$$v_i = \frac{V_{max}[A]}{K_m + [A]} \tag{11}$$

The first-order rate constant $k = V_{max}/K_m = k_{cat}[E]_T/K_m$ was also determined at $[A]_0 < K_m/10$ by fitting reaction time courses, followed for >3 half-lives, to the following equation, in which A, A_0, and A_∞ are absorbances at times t, 0, and infinity, respectively:

$$A = (A_0 - A_\infty)e^{-kt} + A_\infty \tag{12}$$

Proton inventory parameters (i.e. C and ϕ_3^T) and β-deuterium secondary isotope effects reported herein are weighted means of means from repetitive measurements that were conducted on various days. Weighted means were calculated according to the following equation:

$$\bar{X} = \sum_{i=1}^{n} W_i X_i / \sum_{i=1}^{n} W_i \tag{13}$$

The weighting factors are $W_i = 1/\sigma_i^2$, where σ_i^2 is the square of the standard error of the mean for β-deuterium isotope effects or of the standard errors of the least-squares estimates for proton inventory parameters. The standard error of the mean of means is also calculated as a weighted mean according to eq 13 from the standard errors of the repetitive measurements.

Viscosity Experiments. The viscosities of aqueous buffers in which AChE reactions were conducted were adjusted by adding glycerol, as described by Bazelyansky et al.[2a] The viscosigen glycerol not only slows k_1 and k_2, but also has an inhibitory solvent effect on AChE catalysis. Consequently, as did Bazelyansky et al.,[2a] the rate constants plotted in Figure 2 were adjusted by the degree to which hydrolysis of a slow substrate, in the experiments detailed herein (butyrylthio)choline, was inhibited by glycerol. This was done by dividing observed k_E values for ATCh hydrolysis by the fractional inhibition of BuTCh hydrolysis at the various glycerol concentrations.

Computational Modeling of the Transition State. A model of the transition state was constructed by the following procedure: (1) a model of the tetrahedral intermediate for CH_3O^- addition to the carbonyl-protonated form of ATCh was constructed by using the Spartan[29] program; (2) the dihedral angles for the C−S−CH_2−CH_2 and S−CH_2−CH_2−N substructures of the model were constrained at 180°, in accord with the preference of AChE for binding of the fully extended conformation of the substrate;[30] (3) the Spartan model was then geometry optimized by using the Gaussian 94 program and the 6-31+G** basis set,[20] albeit with these dihedral angle constraints; (4) the bond length in the transition state of the methoxy oxygen−carbonyl carbon bond was calculated according to eq 10; and (5) a model of the transition state was generated in a subsequent Gaussian 94 geometry optimization, albeit with the methoxy oxygen−carbonyl carbon bond length and dihedral angle constraints outlined above. This general procedure was also followed for the carbonyl-unprotonated form of ATCh. In this case, however, the tetrahedral adduct was less stable than the products, methyl acetate and thiocholine zwitterion. Because the intrinsic β-deuterium secondary isotope effects suggest that the

(26) (a) Vellom, D. C.; Radić, Z.; Li, Y.; Pickering, N. A.; Camp, S.; Taylor, P. *Biochemistry* **1993**, *32*, 12−17. (b) Radić, Z.; Pickering, N. A.; Vellom, D. C.; Camp, S.; Taylor, P. *Biochemistry* **1993**, *32*, 12074−12084.

(27) (a) Shafferman, A.; Velan, B.; Ordentlich, A.; Kronman, C.; Grosfeld, H.; Leitner, M.; Flashner, Y.; Cohen, S.; Barak, D.; Ariel, N. *EMBO J.* **1992**, *11*, 3561−3568. (b) Ordentlich, A.; Kronman, C.; Barak, D.; Stein, D.; Ariel, N.; Marcus, D.; Velan, B.; Shafferman, A. *FEBS Lett.* **1993**, *334*, 215−220.

(28) Nair, H. K.; Lee, K.; Quinn, D. M. *J. Am. Chem. Soc.* **1993**, *115*, 9939−9941.

(29) Deppmeier, B. J.; Driessen, A. J.; Hehre, W. J.; Johnson, J. A.; Klunzinger, P. E.; Lou, L.; Yu, J.; Baker, J.; Carpenter, J. E.; Dixon, R. W.; Fielder, S. S.; Johnson, H. C.; Kahn, S. D.; Leonard, J. M.; Pietro, W. J.;, SPARTAN SGI Version 5.0.2; Wavefunction Inc.: Irvine, CA, 1997.

(30) Harel, M.; Quinn, D. M.; Nair, H. K.; Silman, I.; Sussman, J. L. *J. Am. Chem. Soc.* **1996**, *118*, 2340−2346.

(31) Ordentlich, A.; Barak, D.; Kronman, C.; Ariel, N.; Segall, Y.; Velan, B.; Shafferman, A. *J. Biol. Chem.* **1998**, *273*, 19509−19517.

(32) A preliminary account of the work described in this paper was reported in the following reference: Malany, S.; Sikorski, R. S.; Seravalli, J.; Medhekar, R.; Quinn, D. M.; Radić, Z.; Taylor, P.; Velan, B.; Kronman, C.; Shafferman, A. In *Structure and Function of Cholinesterases and Related Proteins*; Doctor, B. P., Taylor, P., Quinn, D. M., Rotundo, R. L., Gentry, M. K., Eds.; Plenum Press: New York and London, 1998; pp 197−202.

(33) **Note Added in Proof:** Since the submission of this paper, work has begun on computational models of the tetrahedral intermediate and transition state in which electrophilic interaction at the carbonyl oxygen is provided by three water molecules. The tetrahedral intermediate is more exploded than the corresponding intermediate described in Table 2. For example, the C_1−O_2 and C_1−S distances are 1.413 and 1.971 Å, respectively. Moreover, bond angles about the carbonyl carbon that include sulfur are closely similar to (e.g. O_1−C_1−S = 110.51°) or are smaller than (e.g. O_2−C_1−S = 101.34°) those of the tetrahedral intermediate model of Table 2. A transition state model was generated by constraining the C_1−O_2 distance at 1.48 Å, calculated according to eq 10 with $f = 0.76$ and $D(1) = 1.413$ Å; this procedure is the same as that used to generate the transition state model described in Table 2 and Figure 3. As before, this new transition state model bears appreciable structural similarity to its cognate tetrahedral intermediate, particularly with respect to bond angles in which the carbonyl carbon is the central atom.

transition state closely resembles the tetrahedral intermediate, these computational comparisons indicate that the tripartite oxyanion hole of AChE[30,31] provides the stabilization needed for the tetrahedral intermediate to form.[32,33]

(34) Quinn, D. M.; Seravalli, J.; Nair, H. K.; Medhekar, R. A.; Husseini, B.; Radić, Z.; Vellom, D. C.; Pickering, N.; Taylor, P. In *Enzymes of the Cholinesterase Family*; Quinn, D. M., Balasubramanian, A. S., Doctor, B. P., Taylor, P., Eds.; Plenum Press: New York and London, 1995; pp 203−208.

Acknowledgment. We acknowledge the technical assistance of Rohit Medhekar. This work was supported by NIH grant NS21334 to D.M.Q., NIH grant GM18360 to P.T., and by a contract to A.S. from the US Army Research and Development Command (DAMD17-96-C-6088). S.M. acknowledges the support of a predoctoral fellowship from the University of Iowa Center for Biocatalysis and Bioprocessing.

JA9933590